Haitao Liu*, Yanchong Yu, Weiqing Chen, Qingxian Wang and Guangshun Wang

Effect of Mn/S Ratio on the Hot Ductility of Eco-friendly Bi-S based Free Cutting Steel

Abstract: The hot ductility of eco-friendly Bi-S based free cutting steels with different Mn/S ratios was studied using a Gleeble-1500 thermal–mechanical simulator. The hot ductility of the steel was found to depend on the Mn/S ratio, and the Mn/S ratio of the steel should be greater than 3.5 for hot rolling of billets without crack development. The low Mn/S ratio would inhibit the occurrence of the dynamic recrystallization and cause the formation of the low melting point sulfide Fe-rich (Fe,Mn)S as secondary phases, which could obviously reduce the strength of the grain boundary and resulted in the formation of cracks along the grain boundary. The higher the Mn/S ratio in the steel, the lower the Fe content in the Fe-rich (Fe,Mn)S phases. When the Mn/S ratio in the steel was high enough, the sulfide phases in the steel were mainly MnS as primary inclusions and the low melting point sulfide phases could be effectively avoided forming. While the Mn/S ratio could influence the hot ductility of the steel over the whole temperature range of 900–1200 °C, the segregation of bismuth along grain boundary could be harmful to the hot ductility in addition to the lower Mn/S ratio for the temperature was no more than 1050 °C.

Keywords: free-cutting steel, hot ductility, Mn/S ratio, bismuth, sulfide phases

PACS® (2010). 81.40.-z

***Corresponding author: Haitao Liu:** State Key Laboratory of Advanced Metallurgy, and School of Metallurgical and Ecological Engineering, University of Science and Technology Beijing, Beijing 100083, China. E-mail: liuhaitao1204@126.com
Yanchong Yu, Weiqing Chen: State Key Laboratory of Advanced Metallurgy, and School of Metallurgical and Ecological Engineering, University of Science and Technology Beijing, Beijing 100083, China
Qingxian Wang, Guangshun Wang: Qingdao Iron and Steel Group Co., Ltd., Qingdao 266043, China

1 Introduction

Since the use of the environmentally detrimental Pb-S based free cutting steel was limited, an eco-friendly Bi-S based free cutting steel has been developed, in which lead is replaced by bismuth [1–4]. The Bi-S based steels have similar excellent machinability compared to the Pb-S based steels because bismuth and lead have similar physical properties [3–6].

Unfortunately, eco-friendly Bi-S based free cutting steels are not yet widely used for commercial purpose because their hot rolling is more difficult than that of the Pb-S based free cutting steels [7–12]. The steels were reported to have relatively low ductility to restrict the hot working temperature range, which could induce the cracking during hot rolling [9–12]. The poor hot workability has generally been associated with the Mn/S ratio, but few studies have been done about the effect of Mn/S ratio on the hot ductility of the steels with high sulfur content [13–14]. In this paper, a critical Mn/S ratio for the eco-friendly Bi-S based free cutting steel has been established by hot tensile test, which is in good agreement with the theoretical deduction results from literature [15], and the mechanism of the effect of Mn/S ratio on the hot ductility of the steel has also been investigated in relation to the microstructural changes.

2 Experimental procedures

The tested steels with different Mn/S ratios were melted in a vacuum induction furnace at a temperature of 1580 °C. Pure Bi and ferromanganese alloys lines on a pure iron wire was inserted into the liquid steel by a feeding device of the furnace after melting, then refined for 2 min, when the temperature and composition were uniform, the molten steel was cast to a 6.5 kg ingot with a pouring temperature 1560 °C. The ratio of Mn/S was set to the varing range from 1 to 4 in order to find the critical value for the Bi-S based free cutting steel to improve the hot ductility of these steels. The chemical compositions are shown in Table 1.

These ingots were first reheated at 1200 °C for 2 h in a heating furnace, and then, an air forging hammer was used to forge them into wire rods with a diameter of 15 mm. During the forging process, the temperature was always >1050 °C, and finally, the wire rods were air cooled to room temperature. Specimens with a dimension of

Table 1: Chemical compositions of tested steels, mass%

Steels	C	Si	Mn	S	P	Bi	Mn/S ratio
1	0.07	0.06	0.41	0.34	0.054	0.10	1.21
2	0.08	0.09	0.92	0.31	0.055	0.17	2.97
3	0.08	0.02	1.28	0.35	0.068	0.15	3.66
4	0.07	0.01	1.25	0.31	0.050	0.17	4.03

10 mm diameter and 120 mm length for hot tensile testing were prepared from these wire rods.

The hot tensile test was performed with a Gleeble-1500 thermal-mechanical simulator under argon protection atmosphere, using a constant strain rate of 10^{-2} s^{-1} in the range of 850–1200 °C with an interval of 50 °C. The specimens were first heated to 1350 °C with a heating rate of 10 °C s^{-1} and held for 5 min, then cooled to each testing temperature with a cooling rate of 3 °C s^{-1} and held for 1 min before the tensile testing. After rupture, the samples were immediately quenched by water spraying to maintain the microstructure at the testing temperature, and the reduction in area (R_A) was measured to evaluate their hot ductility.

The fracture surfaces of these steels were observed through a scanning electron microscope (SEM). The longitudinal sections close to the point of fracture were prepared and etched with a picral solution, and then, the microstructures and the inclusions were detected by a combination of the SEM in backscattered electron (BSE) mode and secondary electron (SEI) mode, and the energy dispersive X-ray spectroscopy (EDS).

3 Results and discussion

3.1 Effect of Mn/S ratio on hot ductility

The R_A of all tested steels with different Mn/S ratios in the testing temperature range is shown in Fig. 1. The hot ductility of Bi-S based free cutting steel was found to depend on the Mn/S ratio. The steels showed the largest hot ductility at the ratio of 3.66 and 4.03, while the R_A was obviously increased with the increase of the Mn/S ratio for the ratio in the steel was less than 3.66. Meanwhile, the Mn/S ratio could influence the hot ductility of the steel over the whole temperature range of 900–1200 °C, for example, the hot ductility of steel 1 with the ratio of 1.21 was all very bad over this range. The R_A of steel 4 was lower than that of steel 3 at 850–1000 °C even though it has a higher Mn/S ratio which might be attributed to the higher bismuth

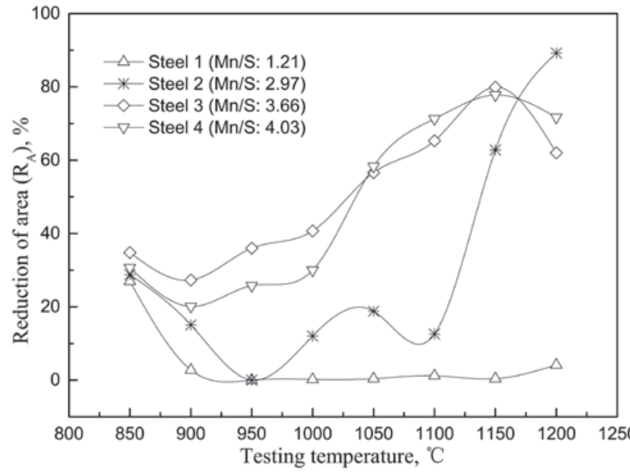

Fig. 1: Hot ductility curves of all tested steels

content of steel 4, because bismuth in the steel also had a detrimental influence on the hot ductility mainly in this temperature range.

Gonzalo and Oscar et al. suggested that there was a critical Mn/S ratio, which could be considered as a border between good and bad results of hot ductility of steels, and this critical value depended on the S content of the steel [15]. A comparison between the experimental Mn/S ratio in this work and the theoretically deduced critical Mn/S ratio by Gonzalo and Oscar et al. is shown in Fig. 2. It can be seen that the agreement between the experimental results in this work and the theoretical deduction by Gonzalo and Oscar et al. was well when the S content of the steel was in the range of 0.30–0.35 wt-%, and the value of the critical ratio at this time was about 3.5. Therefore,

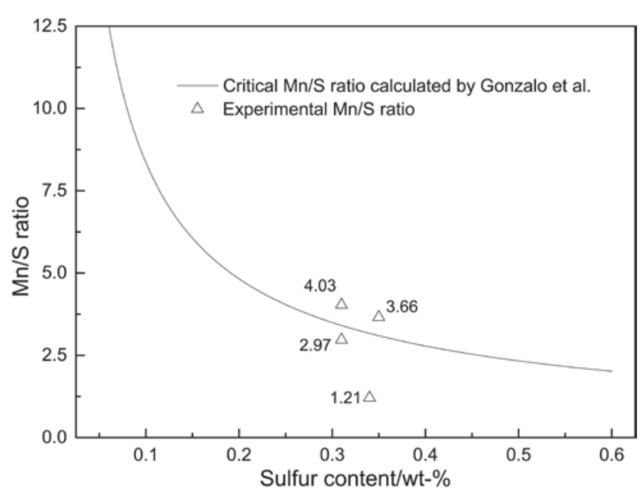

Fig. 2: A comparison between the experimental Mn/S ratio in this work and the theoretically deduced critical Mn/S ratio by Gonzalo and Oscar et al. [15]

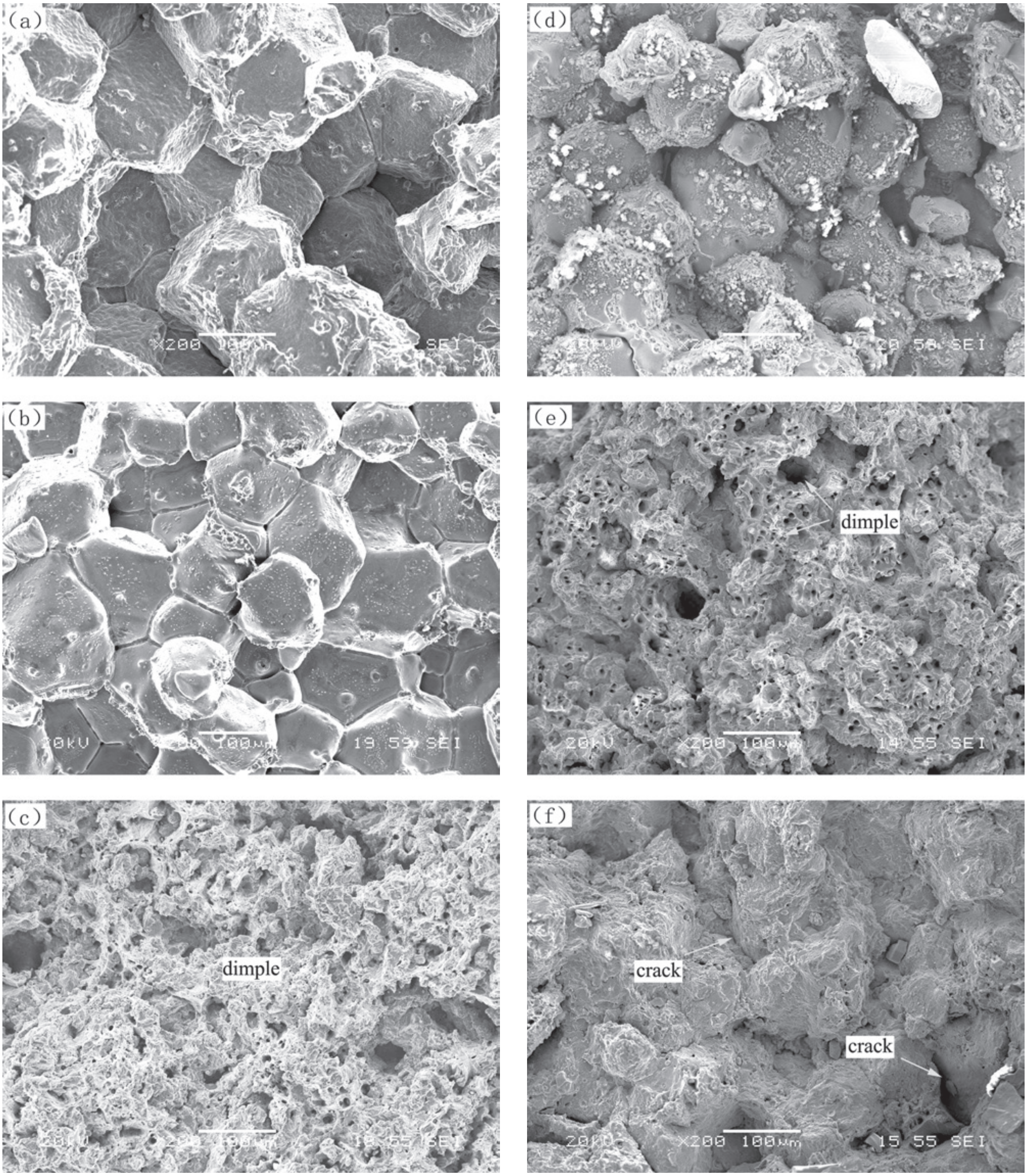

Fig. 3: Fracture morphology of tensile tested samples: (a) steel 1 at 1150 °C; (b) steel 1 at 1000 °C; (c) steel 2 at 1150 °C; (d) steel 2 at 1000 °C; (e) steel 4 at 1150 °C; (f) steel 4 at 1000 °C

the Mn/S ratio of the eco-friendly Bi-S based free cutting steel, in which the S content is around the range of 0.30–0.35 wt-%, should be greater than 3.5 for hot rolling of billets without crack development.

3.2 Fracture morphology

The fracture surfaces of the tensile test specimens were observed by SEM. The steels with good hot ductility all exhibited ductile dimple fractures, but intergranular brittle fractures when the hot ductility was poor. The typical fracture surfaces of the tensile test specimens are shown in the SEM photos (Fig. 3). The fractures of steel 1 at 1150 and 1000 °C both exhibited intergranular brittle failure (Fig. 3a and b), which could indicate that the grain boundary strength of the steel with low Mn/S ratio was lower. Steels 2 and 4 at 1150 °C both showed a ductility failure (Fig. 3c and e), but their fractures at 1000 °C were mainly intergranular (Fig. 3d and f), which agrees with the values of the hot ductility given in Fig. 1.

3.3 Effect of Mn/S ratio on dynamic recrystallization

The flow stress curves for steels 1, 2, and 4 are shown in Fig. 4. The temperature for the onset of dynamic recrystallization (DRX) can generally be obtained from the flow stress curves by noting the first test temperature at which load fluctuations occur in the austenite, because the occurrence of DRX will provide an additional softening to offset part of the work hardening caused by deformation [16–18]. Mintz and Mohamed have reported that DRX is essential for good ductility, and the ductility for high S steel improves only at higher temperatures when DRX is well established [17–20]. From the examination of the flow stress curves in relation to the hot ductility curves in this work, it can be seen that there was no DRX occurring for steel 1 in the whole testing temperature range, but the onset temperatures of DRX for steels 2 and 4 were 1150 and 1100 °C respectively. The Mn/S ratio had a remarkable effect on the onset of DRX, the higher the Mn/S ratio, the lower the onset temperature of DRX. Meanwhile, the recovery temperature of the hot ductility for these steels agreed with the onset of DRX in this work. DRX, i.e. grain boundary migration, can move grain boundaries away from microcracks, leading to the isolation of microcracks and preventing their coalescence at grain boundaries [16–22].

3.4 Generation of sulfide inclusions with different Mn/S ratios

The typical longitudinal microstructures of the quenched fractures for steel 1 with the Mn/S ratio of 1.21 were observed using SEM and EDS, and the result was shown in Fig. 5. A lot of precipitated phases were observed at the grain boundary. EDS analysis of these precipitated phases revealed that they were Fe-rich (Fe,Mn)S phases

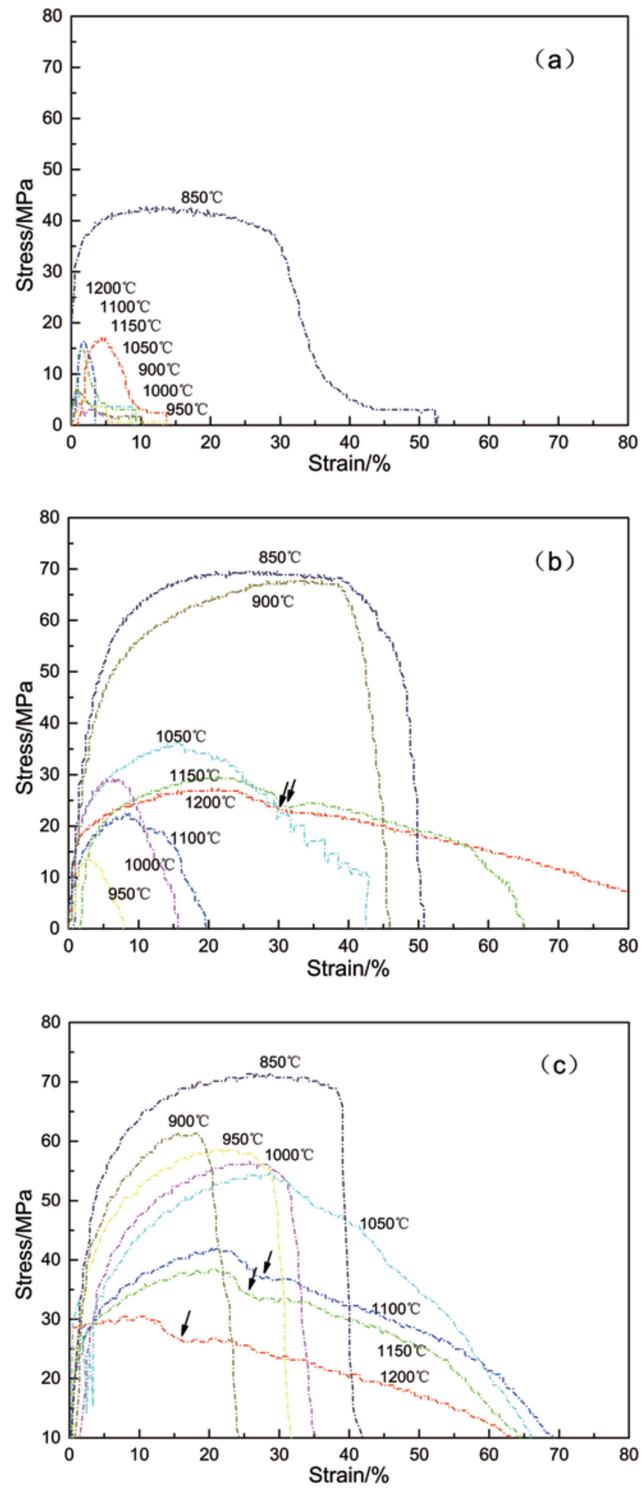

Fig. 4: Flow stress–strain curves as function of tensile temperature for the examined steels (arrows indicate dynamic recrystallization): (a) steel 1; (b) steel 2; (c) steel 4

or FeS phases, which have a low melting point [23]. Meanwhile, from Figs. 3a, 3b and 4a, it can also be seen that the strength of steel 1 was so poor and this result was mainly caused by the weak grain boundary. In other

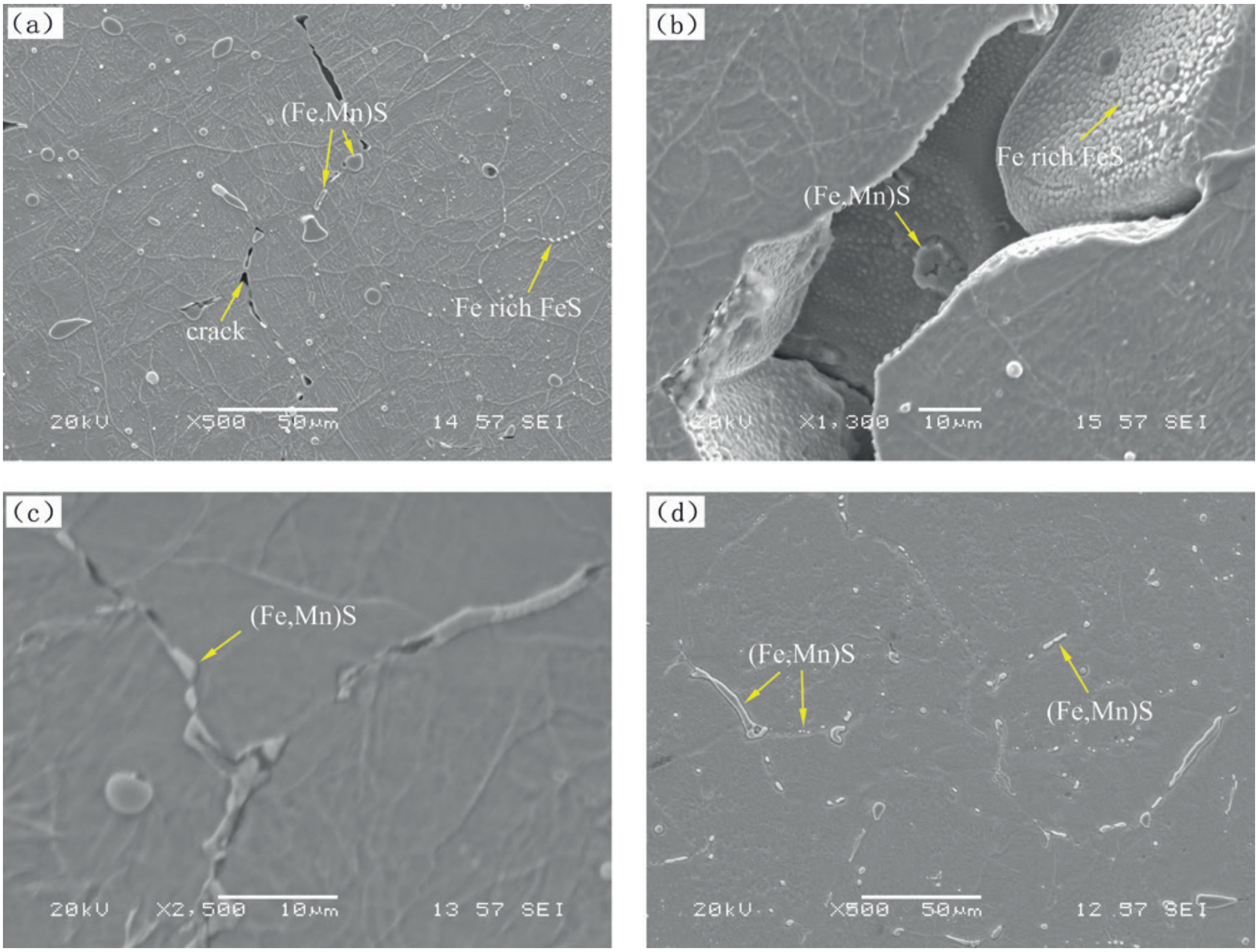

Fig. 5: Typical longitudinal microstructures of quenched fractures for steel 1: (a) microstructure near fracture at 1200 °C; (b) cracks magnification at 1200 °C; (c) microstructure near fracture at 1150 °C; (d) microstructure near fracture at 1100 °C

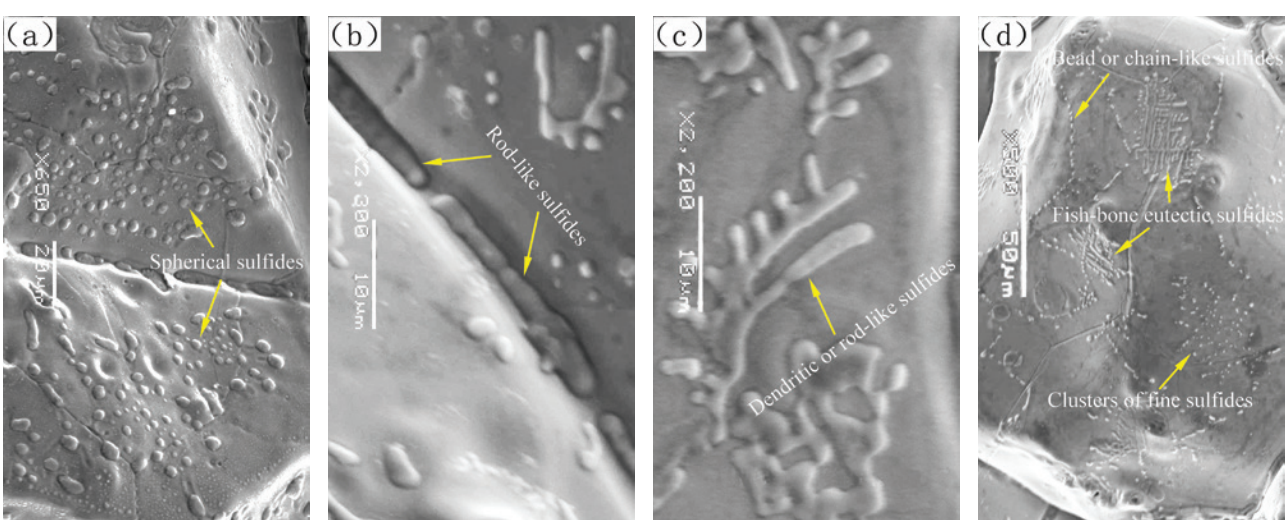

Fig. 6: Typical morphologies of the sulfide inclusions on the surface of fractures in steel 1: (a) spherical sulfides; (b) rod-like sulfides; (c) dendritic or rod-like sulfides; (d) bead or chain-like, fish-bone eutectic, and clusters of fine sulfides

words, these phases with low melting point would obviously reduce the strength of the grain boundary and resulted in the formation of cracks along the grain boundary [24].

As it is known, most of the sulfide inclusions usually precipitate as MnS in the enriched interdendritic liquid at the last stage of solidification during freezing [23–27]. However, the data in the phase diagram of Fe-rich Fe-Mn-S system also shows that an insufficient addition of Mn to S containing steels would cause the formation of the liquid phase or Fe-rich sulfide phase in a peritectic or a eutectic mode [28–30]. In addition, the segregation of sulphur in the steel would promote the formation of the Fe-rich sulfide phases along the grain boundary [28–29]. Therefore, in this work, few MnS as primary sulfide inclusions were formed but many Fe-rich (Fe,Mn)S as secondary sulfide phases after the primary crystallization of the Fe phase during solidification, which would be attributed to the low Mn/S ratio in steel 1. Meanwhile, the morphology of these Fe-rich (Fe,Mn)S phases could be mainly classified to six types as follows: spherical, rod-like, dendritic or rod-like, bead or chain-like, fish-bone eutectic, and clusters of fine sulfides [26–27]. The typical morphologies of them were shown in Fig. 6.

Fig. 7 showed the SEM and EDS photos of the sulfide inclusions which formed in sequence in steel 1 at 1000 and 900 °C. From Fig. 7, it also can be seen that there was a higher Fe content in the Fe-rich sulfide phases precipitated later.

The typical longitudinal microstructures of the quenched fractures for steel 2 with the Mn/S ratio of 2.97 were shown in Fig. 8. It can be seen that there were few Fe-rich sulfide phases precipitated at 1150 °C (Fig. 8a), but many bead or chain-like Fe-rich (Fe,Mn)S phases and cracks at 1100 °C along the grain boundary (Fig. 8b) in accord with its worse ductility. Meanwhile, the Fe content

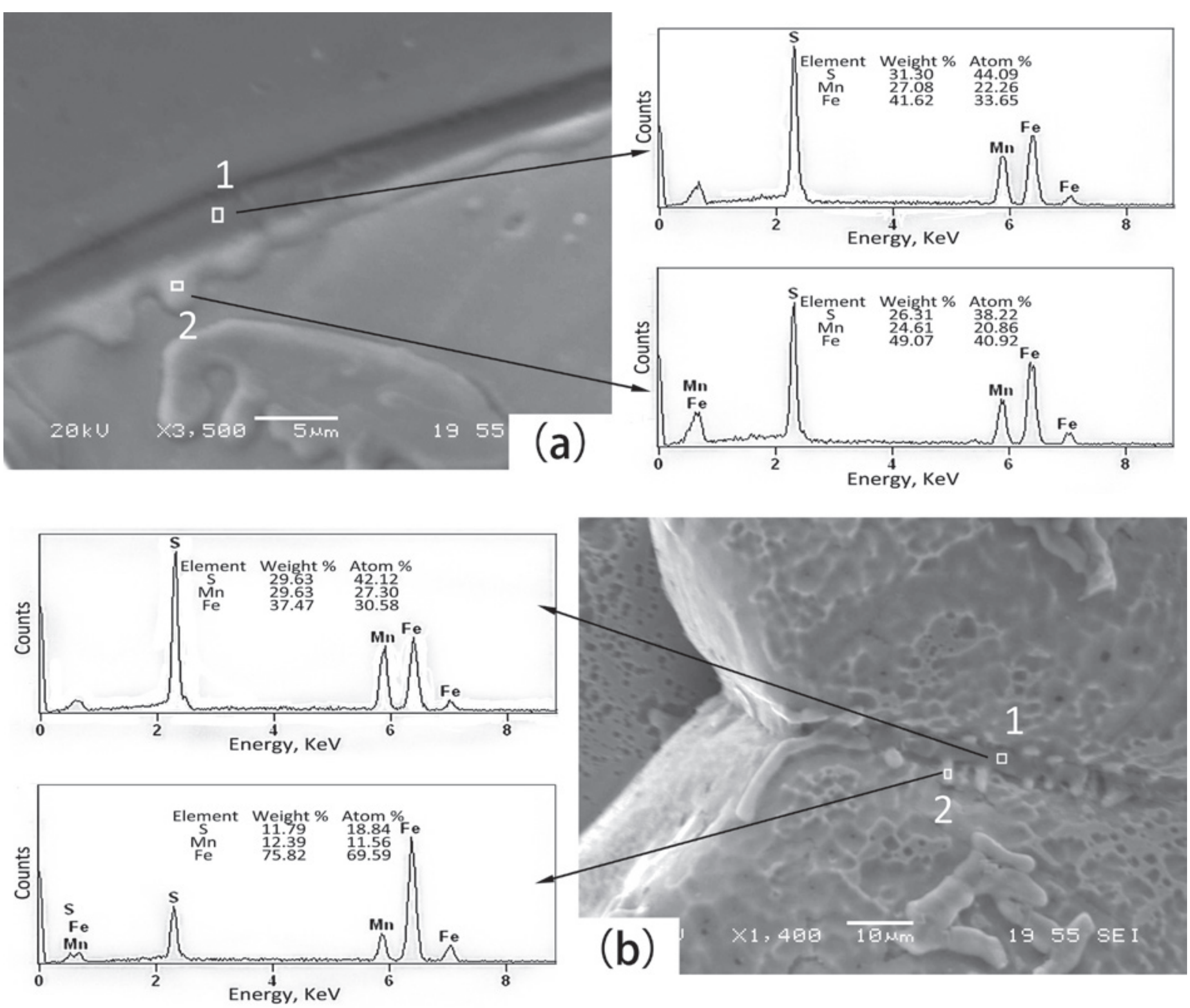

Fig. 7: SEM morphology and EDS analysis of the typical sulfide inclusions formed in sequence for steel 1: (a) 1000 °C; (b) 900 °C

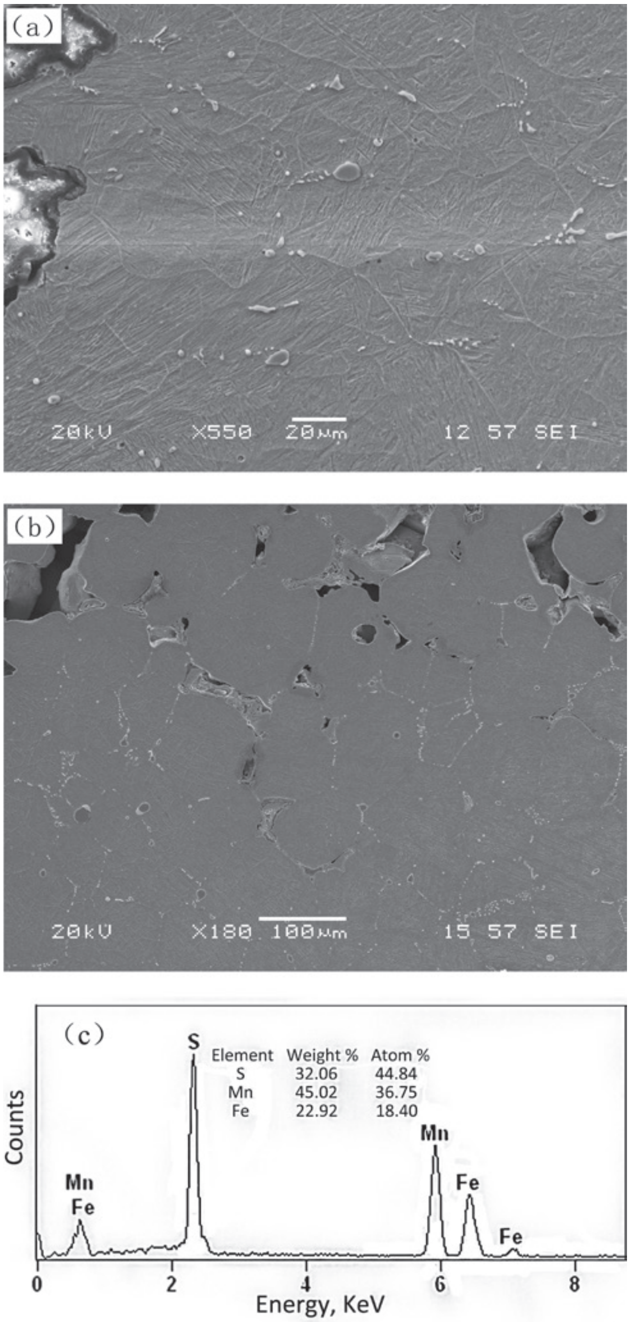

Fig. 8: Typical longitudinal microstructures of quenched fractures for steel 2: (a) microstructure near fracture at 1150 °C; (b) microstructure near fracture at 1100 °C; (c) EDS of sulfide phases

in the Fe-rich (Fe,Mn)S phases was lower compared with that of steel 1 (Fig. 8c), because there was a higher Mn/S ratio in steel 2 and more Mn would combine with S in steel 2.

The typical longitudinal microstructures of the quenched fractures at 1000 °C for steel 4 with the Mn/S ratio of 4.03 were shown in Fig. 5. It can be seen that the sulfide phases in the steel were mainly MnS as primary sulfide inclusions, and a high enough Mn/S ratio could effectively avoid the formation of the low melting point sulfide phases. However, the hot ductility of steel 4 was still poor when the temperature was no more than 1050 °C although the Mn/S ratio of it was high enough. From Figs. 9a and 10b below, it can be seen that the poor hot ductility and the cracks along grain boundary in steel 4 at this time were mainly due to the segregation of bismuth at the grain boundary.

3.5 Grain boundary segregation of bismuth

From the observation and analysis of the longitudinal microstructures of the quenched fractures for steels 2 and 4 using the SEM in SEI and BSE modes. The cracks along austenite grain boundaries accompanied by the segregation of bismuth films had been founded when the testing temperature was no more than 1050 °C in both steels. The typical SEM photos of the bismuth films segregated along austenite grain boundary at 1050 °C for steel 2 and steel 4 were shown in Fig. 10.

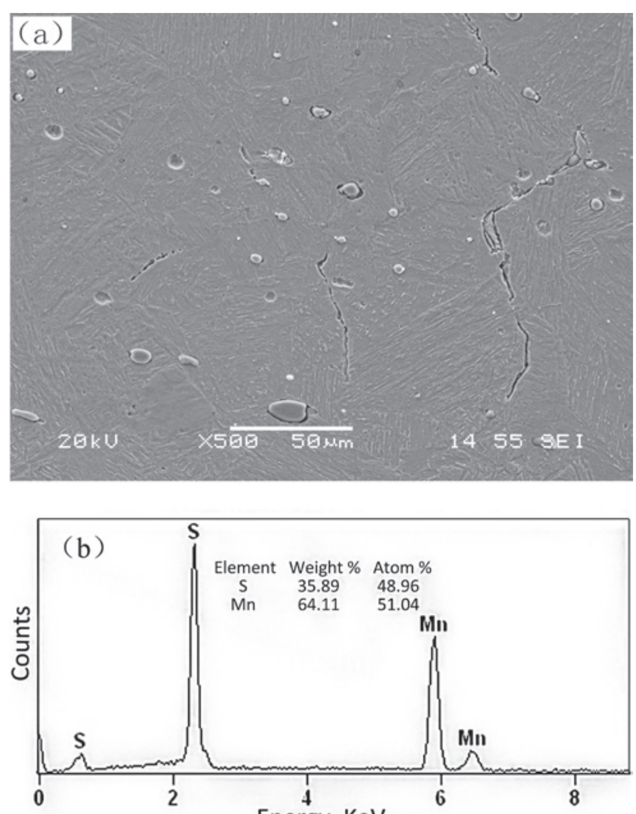

Fig. 9: Typical longitudinal microstructures of quenched fractures at 1000 °C for steel 4: (a) microstructure near fracture; (b) EDS of sulfide phases

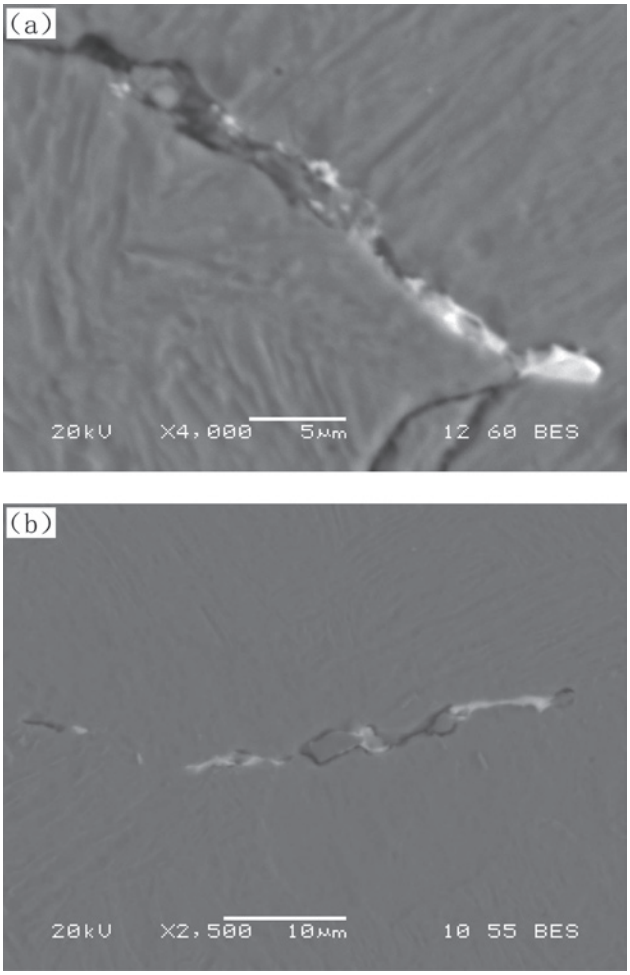

Fig. 10: Typical SEM photos of the bismuth films segregated along austenite grain boundary (BES mode): (a) steel 2 at 1050 °C; (b) steel 4 at 1050 °C

Pure Bi has a melting point of 271.3 °C, the bismuth films present at austenite grain boundary would exist as liquid forms at the testing temperatures and would significantly reduce the strength of the grain boundary and cause grain boundary embrittlement. Therefore, the segregation of bismuth along grain boundary also would be harmful to the hot ductility of the eco-friendly Bi-S based free cutting steel in addition to the lower Mn/S ratio.

4 Conclusions

The hot ductility of the eco-friendly Bi-S based free cutting steel was found to depend on the Mn/S ratio, and the Mn/S ratio of the steel should be greater than 3.5 for hot rolling of billets without crack development.

The low Mn/S ratio could restrain the occurrence of dynamic recrystallization and cause the formation of the Fe-rich (Fe,Mn)S as secondary sulfide phases, these phases with low melting point would obviously reduce the strength of the grain boundary and resulted in the cracks along the grain boundary.

The higher the Mn/S ratio in the steel, the lower the Fe content in the Fe-rich (Fe,Mn)S phases. When the Mn/S ratio in the steel was high enough, the sulfide phases in the steel were mainly MnS as primary sulfide inclusions and the formation of low melting point sulfide phases could be effectively avoided.

While the Mn/S ratio could influence the hot ductility of the steel over the whole temperature range of 900–1200 °C, the segregation of bismuth along grain boundary could be harmful to the hot ductility in addition to the lower Mn/S ratio for the temperature was no more than 1050 °C.

Received: May 24, 2013. Accepted: July 12, 2013.

References

[1] K. Sander, J. Lohse and U. Pirntke, *Heavy Metals in Vehicles – Final Report*, Institut für Ökologie und Politik GmbH, Hamburg, pp. 4–44 (2000).
[2] J. Lohse, K. Sander and M. Wirts, *Heavy Metals in Vehicles II – Final Report*, Institut für Ökologie und Politik GmbH, Hamburg, pp. 45–91 (2001).
[3] R. Philip, B. Volker and E. Ingo, *Steel Res. Int.*, **178**(12), 908–914 (2007).
[4] M. Somekawa, M. Kaiso and Y. Matsushima, *Kobelco Technology Review*, **24**(1), 9–13 (2001).
[5] L. Vea, *SAE Technical Paper on 'New Steel Bar Products and Processing for Automotive Applications'*, Society of Automotive Engineers, Detroit, pp. 77–82 (1997).
[6] H.T. Liu and W.Q. Chen, *Steel Res. Int.*, **83**(12), 1172–1179 (2012).
[7] J. Klapsia, *Hutnicke Listy*, **58**(9), 18–19 (2003).
[8] J. Klapsia and E. Karczmarczyk, *Hutnicke Listy*, **55**(10), 36–38 (2000).
[9] Y. Kim, H. Kim, S.Y. Shin, K. Rhee, S.B. Ahn, D.L. Lee, N.J. Kim and S. Lee, *Metall. Mater. Trans. A*, **42**, 3095–3105 (2011).
[10] S.K. Cho, *J. Korean Inst. Met. Ma.*, **34**(7), 822–829 (1996).
[11] H. Kim, M. Kang, S.Y. Shin and S. Lee, *Mat. Sci. Eng. A*, **568**, 8–19 (2013).
[12] Y. Kim, H. Kim, S.Y. Shin, K. Rhee, S.B. Ahn, D.L. Lee, N.J. Kim and S. Lee, *Metall. Mater. Trans. A*, **43**(3), 882–892 (2012).
[13] K. Oikawa, H. Ohtani, K. Ishida and T. Nishizawa, *ISIJ Int.*, **35**(4), 402–408 (1995).
[14] L.K. Bigelow and M.C. Flemings, *Metall. Mater. Trans. B*, **6**(2), 275–283 (1975).
[15] G.A. Toledo, O. Campo and E. Lainez, *Steel Research*, **64**(6), 292–299 (1993).
[16] E. López-Chipres, C. Maldonado, A. Bedolla-Jacuinde, M. El-Wahabi and J.M. Cabrera, *Mat. Sci. Eng. A*, **480**(1), 49–55 (2008).

[17] B. Mintz, R. Abushosha and J.J. Jonas, *ISIJ Int.*, **32**(2), 241–249 (1992).
[18] B. Mintz and Z. Mohamed, *Mater. Sci. Technol.*, **4**(10), 895–902 (1988).
[19] A. Cowley and B. Mintz, *Mater. Sci. Technol.*, **20**(11), 1431–1439 (2004).
[20] B. Mintz, R. Abu-Shosha and M. Shaker, *Mater. Sci. Technol.*, **9**(10), 907–914 (1993).
[21] F. Zarandi and S. Yue, *Metall. Mater. Trans. A*, **37**(7), 2316–2320 (2006).
[22] E. López-Chipres, C. Maldonado, A. Bedolla-Jacuinde and J.M. Cabrera, *Mat. Sci. Eng. A*, **460**, 464–470 (2007).
[23] G. Sridhar, S.K. Das and N.K. Mukhopadhyay, *Eng. Fail. Anal.,* **6**(3), 155–172 (1999).
[24] C. Zhang, E.B. Yue and S.T. Qiu, *Continuous Casting*, **27**(6), 6–10 (2008).
[25] Z.Z. Liu, M. Kuwabara, R. Satake and T. Nagata, *ISIJ Int.*, **49**(7), 1087–1093 (2009).
[26] L.K. Bigelow and M.C. Flemings, *Metall. Mater. Trans. B*, **6**, 275–283 (1975).
[27] E.T. Turkdogan, *Metall. Mater. Trans. B*, **6**, 663–664 (1975).
[28] H. Ohtani, K. Oikawa and K. Ishida, *High Temp. Mat. Processes*, 1**9**(3), 197–210 (2000).
[29] G.S. Mann and L.H. Van-Vlack, *Metall. Mater. Trans. B*, **7**, 469–475 (1976).
[30] J. Miettinen and B. Hallstedt, *Calphad*, **22**(2), 257–273 (1998).